

SYNTHESIS, CHARACTERIZATION, ANTIMICROBIAL STUDIES, AND MOLECULAR DOCKING STUDIES OF TRANSITION METAL COMPLEXES FORMED FROM A BENZOTHAZOLE-BASED AZO LIGAND

Saud I. Al-Resayes¹, Amer J. Jarad², Jinan M. M. Al-Zinkee³, Taghreed H. Al-Noor^{2*}, Marei M. El-ajaily⁴, Mohnad Abdalla⁵, Kim Min⁶, Mohammad Azam^{1*}, Ranjan K. Mohapatra^{7*}

¹Department of Chemistry, College of Science, King Saud University, Riyadh, 11451, Saudi Arabia

²Department of Chemistry, College of Education for Pure Science / Ibn-Al-Haitham, University of Baghdad, Iraq

³Department of Chemistry, College of Science, University of Diyala, Iraq

⁴Department of Chemistry, Faculty of Science, University of Benghazi, Benghazi, Libya

⁵Key Laboratory of Chemical Biology (Ministry of Education), Department of Pharmaceutics, School of Pharmaceutical Sciences, Cheeloo College of Medicine, Shandong University, 44 Cultural West Road, Shandong Province 250012, PR China

⁶Department of Safety Engineering, Dongguk University, 123 Dongdae-ro, Gyeongju 780714, Gyeongbuk, Republic of Korea

⁷Department of Chemistry, Government College of Engineering, Keonjhar, Odisha, India

(Received December 26, 2022; Revised March 31, 2023; Accepted April 1, 2023)

ABSTRACT. The azo ligand obtained from the diazotization reaction of 2-aminobenzothiazole and 4-nitroaniline yielded a novel series of complexes with Co(II), Ni(II), Cu(II), and Zn(II) ions. The complexes were investigated using spectral techniques such as UV-Vis, FT-IR, ¹H and ¹³C NMR spectroscopic analyses, LC-MS and atomic absorption spectrometry, electrical conductivity, and magnetic susceptibility. The molar ratio of the synthesized compounds was determined using the ligand exchange ratio, which revealed the metal-ligand ratios in the isolated complexes were 1:2. The synthesized complexes were tested for antimicrobial activity against *S. aureus*, *E. coli*, *C. albicans*, and *C. tropicalis* bacterial species. Additionally, their binding affinities were predicted using molecular docking analysis, and their pharmacokinetic and drug-likeness properties were evaluated.

KEY WORDS: Azo ligand, Metal complexes, Antimicrobial studies, Molecular docking study

INTRODUCTION

Organic molecules with electron donor/acceptor groups containing π -conjugated systems have attracted a lot of interest over the years owing to their unique molecular structure and potential applications [1-6]. Among such compounds, the azo compounds having the C=N=N-C functionality are widely employed as photoactive materials in optics and solar cells, as well as in pharmaceutical and biological research as biochemical sensors, catalysts, and enzyme inhibitors [7-12]. Azo compounds have also been used in coordination chemistry as they display strong chelating ability. The resulting azo ligand-based metal complexes have exceptional thermal stability and have found useful applications in photoelectronics, as dyes in the textile industry, and as scaffolds for the design of new anti-inflammatory, anticancer, and antimicrobial agents [13-17]. In fact, with the rise in antimicrobial drug resistance worldwide, transition metal complexes have gained a lot of attention due to their effectiveness against a range of pathogens [18-21].

*Corresponding author. E-mail: drtaghreed2@gmail.com; azam_res@yahoo.com; ranjank_mohapatra@yahoo.com

This work is licensed under the Creative Commons Attribution 4.0 International License

Over the years, nitrogen-containing heterocycle compounds have been shown to play critical roles in a wide variety of biological functions; as a result, they have risen to prominence as one of the most important families of naturally occurring compounds, with various applications including those in the fields of dyes, high-performance materials, and pharmaceuticals [22]. Among such type of compounds, benzothiazole and its derivatives have been the focus of extensive study for their potential use in a wide range of pharmaceutical drugs, natural products, and synthetic intermediates [23-24]. These compounds not only have medicinal capabilities, but they also have fascinating photophysical properties [23-24].

In light of the broad range of biological applications reported for azo compounds and benzothiazole, as well as complexes with transition metal ions, we report herein the synthesis of a novel series of Co(II), Ni(II), Cu(II) and Zn(II) metal complexed produced from a benzothiazole based azo ligand. All metal-ligand complexes were investigated for their antimicrobial activity. A molecular docking approach was also used to predict the binding affinity of these compounds towards three biological targets including the insulin receptor kinase, the voltage-gated potassium channel KCNQ2, and the sodium-dependent serotonin transporter.

EXPERIMENTAL

Material and methods

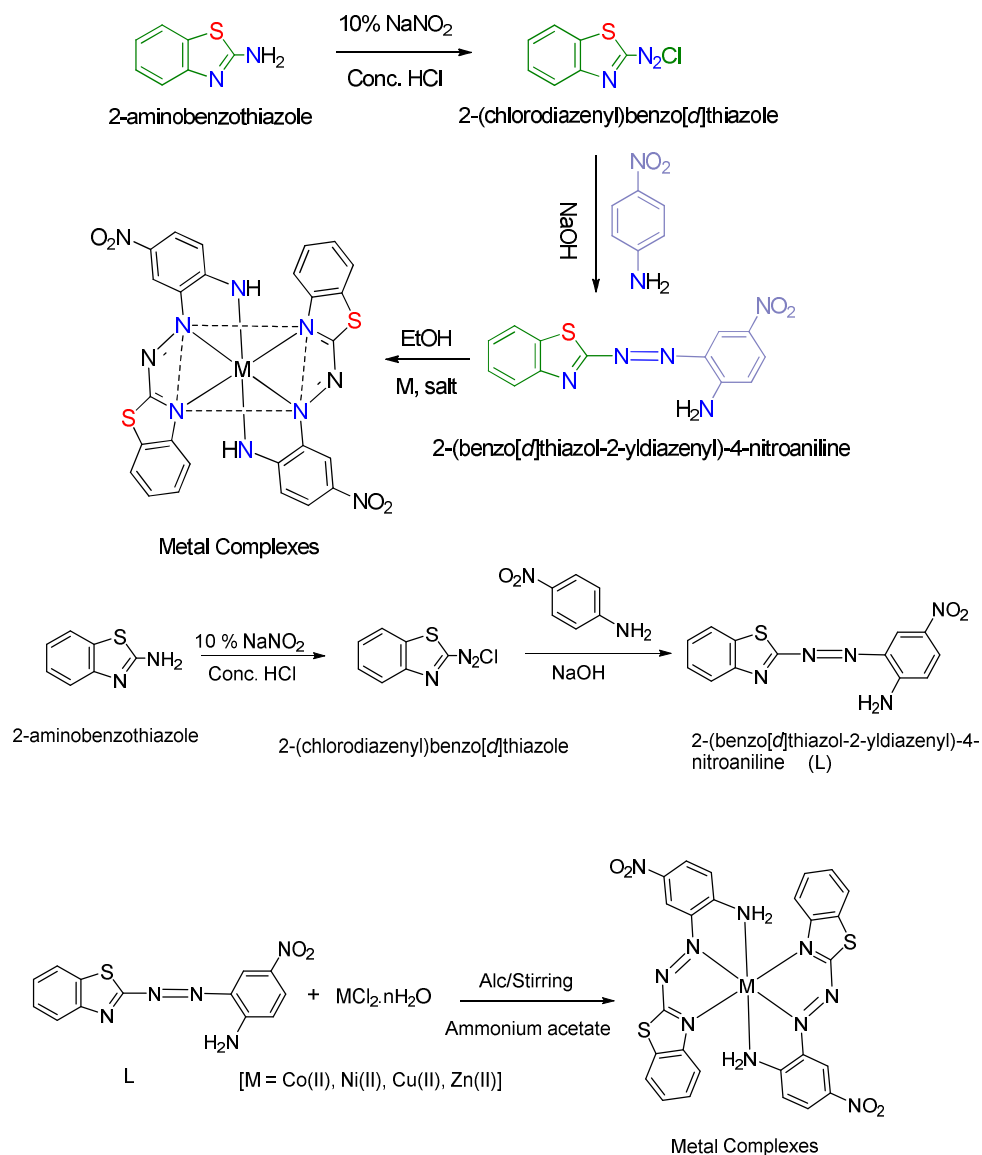
All the chemicals, reagents, and metal salts were used in their original form. A Shimadzu A.A-160A spectrophotometer was used to measure atomic absorption. The ^{13}C and ^1H -NMR spectra were recorded in d_6 -DMSO with TMS as a reference using a Bruker-300 MHz Ultra Shield spectrometer. A Shimadzu UV-160A spectrophotometer was used to record UV-Vis spectra. IR spectra with KBr were taken at $4000\text{--}400\text{ cm}^{-1}$ on a Shimadzu FTIR-8400S Fourier Transform Infrared spectrophotometer. A LC-MS QP50A: Shimadzu-E170EV spectrometer was used to record mass spectra. The conductivity of DMSO (10^{-3} mol/L) was measured at $25\text{ }^\circ\text{C}$ using a Philips PW- Digital Conductivity meter. Magnetic properties were measured using a Sherwood Scientific auto magnetic susceptibility balance at $25\text{ }^\circ\text{C}$.

Preparation of the azo ligand

A mixture of 2-aminobenzothiazole (0.375 g, 1.0 mmol), 2 mL conc. HCl, and 10% NaNO_2 in ethanol was diazotized at $5\text{ }^\circ\text{C}$ as reported in literature [25]. The resulting solution was gradually added to an ethanolic solution of 4-nitroaniline (0.307 g, 1.0 mmol) with continuous stirring at freezing temperature, followed by the addition of 25 mL of 1 M NaOH solution. The result was a slightly brown-colored product that was filtered off and washed with hexane and diethyl ether several times to obtain a pure brown-colored compound, which was filtered, cleaned, and then allowed to dry (Scheme 1).

Preparation of azo ligand-based coordination compounds

The EtOH solution of the azo ligand (0.299 g, 2 mmol) was added drop by drop to the ethanolic solution of the metal salts in 2:1 molar ratio with stirring. To maintain the required pH, ammonium acetate (0.771 g, 0.01 M, 1 L doubly deionized water) was added to the above reaction mixture. The resulting reaction mixture was refluxed for 1 h before cooling until a dark color precipitate was produced, which was filtered, washed, and dried (Scheme 1).



Scheme 1. Synthetic route for the azo ligand and its metal complexes.

Determination of the stability constant and Gibbs free energy

The following equations were used to calculate the stability constant (K) for each metal-ligand complex;

$$K = \frac{1 - \alpha}{4\alpha^3 C^2} ; \quad \alpha = \frac{A_m - A_s}{A_m}$$

where c is the compound's mol/L concentration, and α is the degree of dissociation. A_s denotes absorbance in a solution with the same amount of ligand and metal ion, while A_m denotes absorbance in a solution with the same amount of metal but a surplus of ligand. Large (K) values suggest a high stability for the resulting compounds [26]. The Gibbs free energy (ΔG) was calculated using the following equation [27];

$$\Delta G = -RT \ln k$$

where, R is the gas constant ($8.314 \text{ J.K}^{-1} \text{ mol}^{-1}$) and T is the absolute temperature (in Kelvin).

Antimicrobial activity

In vitro microbial activities were determined from the diameter of clear inhibition zones caused by the studied compounds against *S. aureus*, *E. coli*, *C. albicans* and *C. tropicalis* by the disc diffusion assay. Long-term stability testing of the studied compounds was carried out in dimethylsulphoxide (DMSO) solution. On microorganisms, the ligand and its complexes were tested for microbial activity. Bioactivity was evaluated by assessing the growth inhibition zone and minimum inhibition concentration against test species [28]. The ligand and its complexes showed promising antibacterial and antifungal activity when tested against mentioned species.

Molecular docking study

The 3D crystal structures of the insulin receptor kinase (PDB ID: 1GAG), voltage-gated potassium channel KCNQ2 (PDB ID: 7CR0), and sodium-dependent serotonin transporter (PDB ID: 516X) were obtained from the Protein Data Bank (<http://www.rcsb.org/pdb>). Autodock Vina was used to perform receptor-oriented versatile docking [29] using previously published molecular docking protocols to predict the binding affinities of the compounds under investigation [30].

Pharmacokinetics and drug-likeness predictions

The SwissADME and PubChem online software were used to predict the pharmacokinetic, drug-likeness, solubility, synthetic accessibility, and Lipinski's properties of the investigated compounds. The Ghose, Egan, Veber, and Muegge drug-likeness filters were used to improve the predictions.

RESULTS AND DISCUSSION

Physico-chemical properties of the azo ligand and its metal complexes

The non-electrolytic nature of all the studied compounds was revealed by the molar conductivity data. The chemical composition of all metal-ligand complexes [ML_2] was verified using elemental and spectral data, where $M = \text{Co(II)}$, Ni(II) , Cu(II) , Zn(II) , and $L = \text{azo ligand}$.

NMR analysis

The $^1\text{H-NMR}$ spectrum of the azo ligand showed a range of aromatic protons with signals at δ_{H} 6.67-8.47. The proton signals attributable to $\delta(\text{NH}_2)$ were observed at δ_{H} 6.61. In the synthesized coordination compounds, however, the latter showed deshielding as a result of coordination to the zinc ion. The signal at δ_{C} 149.9 in the $^{13}\text{C-NMR}$ spectrum of the azo ligand was assigned to the carbon atom attached to the amino group, whereas the signal at δ_{C} 151.5 was attributed to the -C-N signal. Various signals in the range δ_{C} 143.0-120.7 were assigned to the carbon atoms of the aromatic ring.

LC-MS analysis

The mass spectrum of the azo ligand (L) revealed a peak at m/z 299.2 corresponding to $C_{13}H_9N_5O_2S$ (Figure 1). The peaks at m/z 206.2, 79.2, and 35, could be attributed most likely to the loss of nitrogen, aromatic, and sulfur groups. The mass spectrum of the zinc-ligand complex showed a peak at m/z 661, which corresponds to the formula $C_{26}H_{16}N_{10}S_2O_4Zn$ (Figure 2). Other peaks at m/z 660.5, 625.3, 605, 572, 472, and 407 may be due to the loss of nitrogen, water, or zinc ions.

Calibration curve and model conditions

To determine the interaction between the studied metal ions and the ligand, the pH, concentration, and wavelength (λ_{max}) were optimized. The various absorbance values (λ_{max}) observed for the studied compounds at various pH levels are shown in Table 1. The absorbance of the studied compounds was constant in a buffer solution made from NH_4OOCCH_3 at pH 5-9 (Figure 3). Several concentrations of mixed aqueous-ethanol ligand and metal ions were measured in the range of 10^{-5} – 10^{-3} mol/L, with the experimental results proving that prepared complexes obeyed Beer's rule at concentrations ranging from 1×10^{-4} mol/L to 3×10^{-4} mol/L and displayed a strong intense color. Plotting absorbance towards molar concentration yielded a straight line with a correlation factor of $R > 0.9980$ (Figure 4).

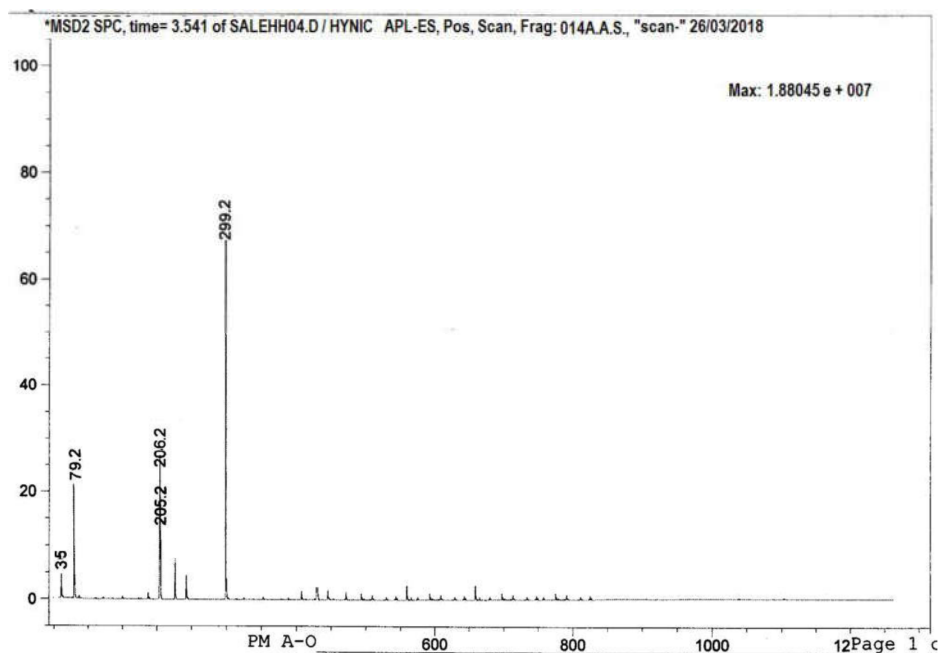


Figure 1. Mass spectrum of the azo ligand (L).

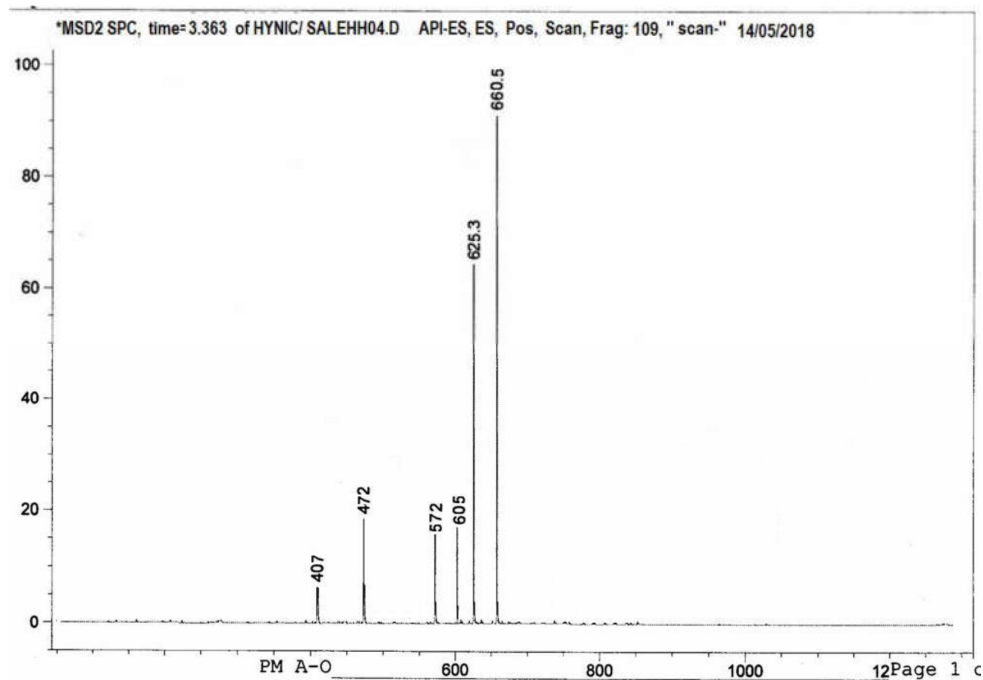


Figure 2. Mass spectrum of the $[Zn(L)_2]$ complex.

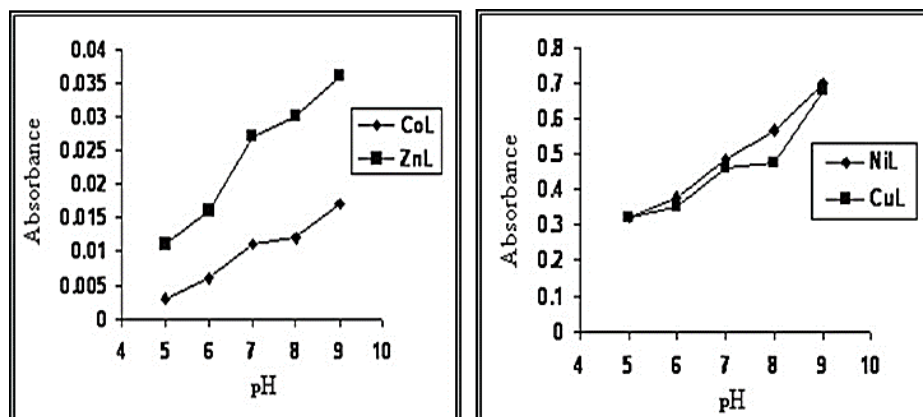


Figure 3. Effect of pH variation on the absorbance (λ_{max}) of the $[ML_2]$ complexes.

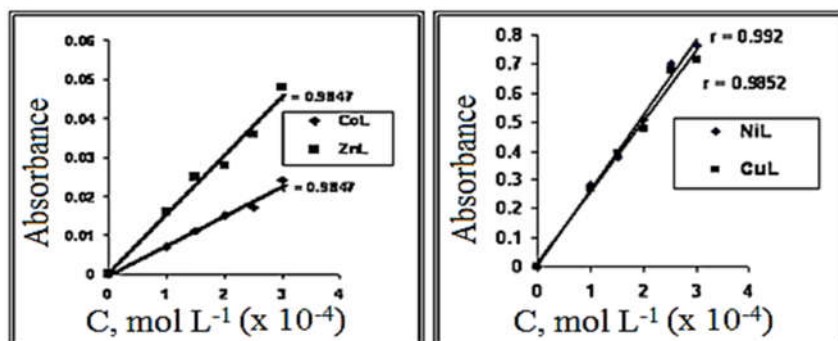


Figure 4. Linear relationship between molar concentration and absorbance obtained for the $[ML_2]$ complexes.

Table 1. UV- Vis and analytical data for the synthesized compounds.

Compounds	Optimum pH	Optimum molar conc. $\times 10^{-4}$	M:L ratio	(λ_{max}) nm	ABS	ϵ_{max} ($L \cdot mol^{-1} \cdot cm^{-1}$)	Λ_m ($S \cdot cm^2 \cdot mol^{-1}$)	μ_{eff} (B.M)
Ligand (L)	-	-	-	218 290 410	2.198 0.785 2.340	2198 785 2340	-	-
$[Co(L)_2]$	9	2.5	1:2	220 278 480 732 886 976	1.738 0.637 1.593 0.007 0.006 0.037	1738 637 1593 7 6 37	12.63	4.85
$[Ni(L)_2]$	9	2.5	1:2	292 478 672 888 978	0.536 1.379 0.005 0.002 0.033	536 1379 5 2 33	13.42	2.91
$[Cu(L)_2]$	9	2.5	1:2	291 414 476 890	1.177 2.255 1.974 0.023	1177 2255 1974 23	17.80	1.73
$[Zn(L)_2]$	9	2.5	1:2	219 288 332 478	1.218 0.617 0.440 1.333	1218 617 440 1333	11.50	Dia.

Metal-to-ligand ratio

The stoichiometry (mole ratio) of the synthesized complexes in solutions was measured at optimized λ_{max} and pH. Using Job's method, the metal ion-to-ligand ratio was found to be 1:2 in all complexes (Figure 5).

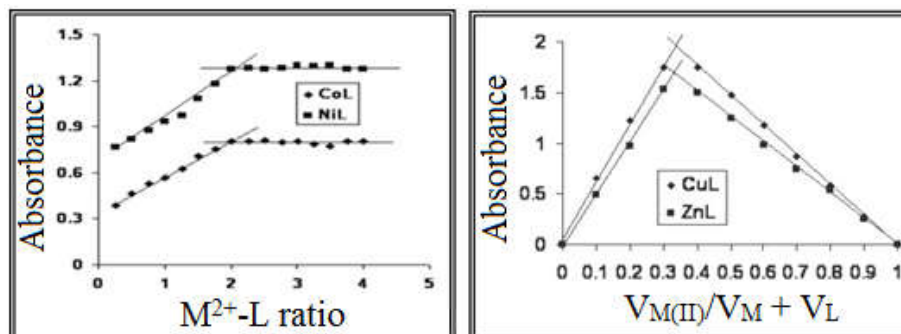


Figure 5. Mole ratio and Job's method evaluation of the $[ML_2]$ complexes.

Physical states

The interaction of the ligand dissolved in ethanol with the metal ions at optimum pH was used to estimate the solid metal complex at a ratio of (1:2) (metal:ligand). The determined values and the results of elemental analysis and metal import from compounds were similar. Compounds dissolved in DMSO (10^{-3} mol/L) had non-electrolytic type conductivity [31] (Table 1).

Determination of stability constant and Gibbs free energy

The reaction between the azo ligand (L) and the metal ions under investigation produced a negative value of (ΔG) (Table 2).

Table 2. Stability constant and Gibbs free energy of the $[ML_2]$ complexes.

Compound	A_s	A_m	α	k	Lin k	ΔG kJ.mol ⁻¹
$[Co(L)_2]$	0.569	0.807	0.295	117.50×10^6	18.581	- 46.035
$[Ni(L)_2]$	0.931	1.274	0.269	182.75×10^6	19.023	- 47.130
$[Cu(L)_2]$	1.466	1.762	0.168	832.00×10^6	20.539	- 50.886
$[Zn(L)_2]$	1.135	1.535	0.260	18.50×10^6	16.733	- 41.457

UV-Vis analysis

Table 1 shows the UV-Vis spectral data of the prepared compounds recorded in ethanol (10^{-3} mol/L). Peaks at 218, 290, and 410 nm in the UV/Vis range of the azo ligand (L) were attributed to a mild energy ($\pi \rightarrow \pi^*$) transition. Peaks at 220, 278, and 480 nm were observed in the Co(II) compound, which were due to intra ligand ($M \rightarrow L$) charge transfer transitions [31]. Peaks at 732, 886, and 976 nm were also allocated to electronic transitions ${}^4T_{1g(F)} \rightarrow {}^4T_{1g(P)}(v_3)$, ${}^4T_{1g(F)} \rightarrow {}^4A_{2g}(v_2)$ and ${}^4T_{1g(F)} \rightarrow {}^4T_{2g(F)}(v_1)$ were also observed in Ni(II) complex exhibiting absorption peaks at 291 nm and 478 nm corresponding to intra ligand and ($M \rightarrow L$) charge transfer transitions, respectively. Electronic transition ${}^3A_{2g} \rightarrow {}^3T_{1g(P)}(v_3)$, ${}^3A_{2g} \rightarrow {}^3T_{1g(F)}(v_2)$ and ${}^3A_{2g} \rightarrow {}^3T_{2g(F)}(v_1)$ was assigned to peaks observed at 672, 888, and 978 nm, respectively. Intra ligand and ($M \rightarrow L$) charge transfer transitions gave rise to peaks at 291, 414, and 476 nm in the Cu(II) complex, while a second peak at 890 nm was attributed to the ${}^2E_g \rightarrow {}^2T_{2g}$ transition [31-32]. The intra ligand ($M \rightarrow L$) charge transfer transitions in the Zn(II) complex exhibited peaks at 219, 288, 332, and 478 nm. Since there was no d-d transition, the magnetic susceptibility indicated diamagnetic nature; hence, it can

be inferred from the above findings that the results are in accordance with the octahedral geometry in all complexes.

FT-IR analysis

The asymmetric and symmetric vibrations due to NH_2 in the azo ligand appeared at 3484 cm^{-1} and 3414 cm^{-1} , respectively [33, 34]. The vibration of the (C=C) group was represented by bands at 1593 cm^{-1} and 1562 cm^{-1} . In the metal complexes, the band at 1446 cm^{-1} due to $\nu(\text{N}=\text{N})$ shifted to a lower wave number, suggesting that it is involved in coordination [33, 34]. The stretching frequency bands for the metal-nitrogen links were observed at $424\text{--}486\text{ cm}^{-1}$.

Antimicrobial activity

The disc diffusion assay was used to test the studied compounds for antimicrobial activity against *S. aureus*, *E. coli*, *C. albicans*, and *C. tropicalis*. The synthesized compounds showed promising activity against *S. aureus* and *E. coli*. In contrast to the free ligand and other complexes, the zinc-ligand complex displayed the highest antibacterial activity, with inhibition zones of 17 mm and 19 mm against *S. aureus* and *E. coli*. None of the compounds were active against *C. albicans* and *C. tropicalis* (Figure 6).

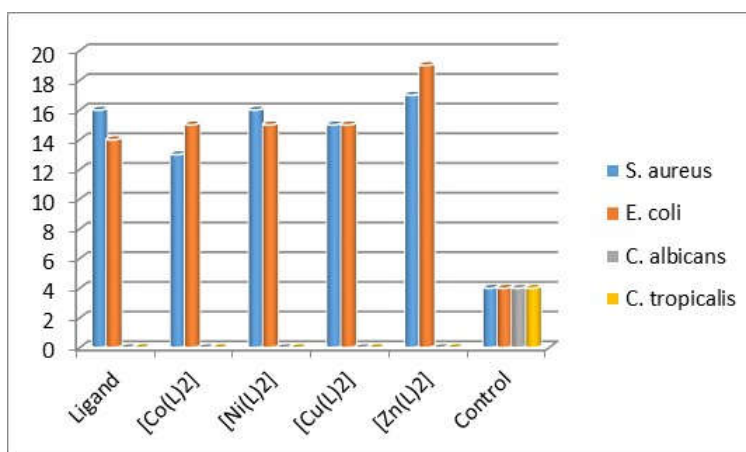


Figure 6. The antimicrobial activities of the compounds were measured in terms of inhibition circle diameter (millimeter) after 24 hours.

Molecular docking study

The binding energy values obtained ranged from -8.6 to -10.7 kcal/mol. In comparison to the free ligand, the metal complexes showed the lowest binding energy with the target proteins. They also showed the highest binding affinity for the voltage-gated potassium channel KCNQ2 (lowest binding energy = -10.7 kcal/mol). The amino acid residues ASP1083, SER1086, GLN1004, LEU1002, ASN1097, LEU248, GLY249, PHE100, PHE104, TYR237, PHE240, PHE297 interact with the investigated compounds. The best docking poses obtained for the studied compounds with each of the selected protein targets are presented in Figure 7.

The insulin receptor is a tyrosine kinase type of protein important for the regulation of cell growth and/or differentiation [35]. The voltage-gated potassium channel KCNQ2 has been

identified as a key target for new drugs to treat epilepsy, pain and other diseases related to neuronal hyper-excitability [36].

The serotonin transporter is a target for antidepressant and psychostimulant drugs [37]. Altogether, these results indicate that the studied compounds may have applications as new therapeutic agents, which remains to be explored further.

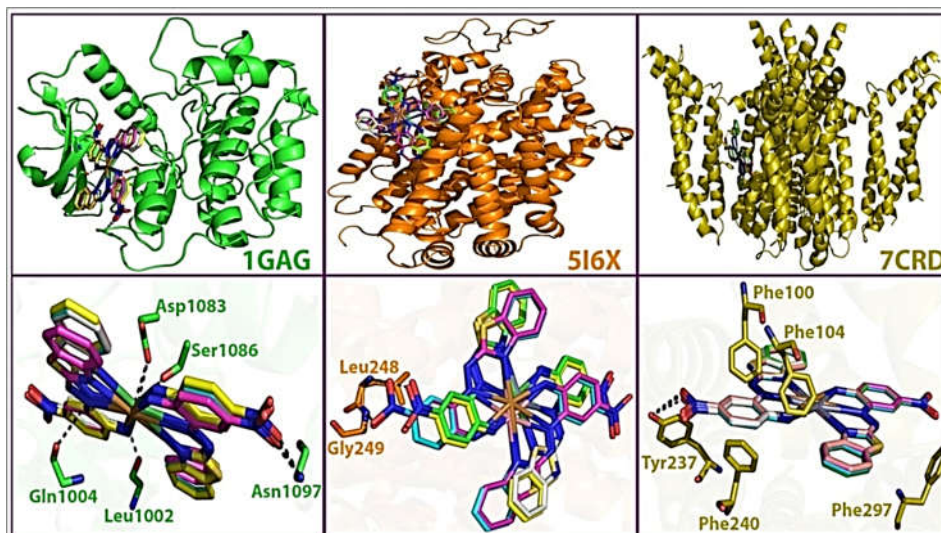


Figure 7. The best docking poses of the compounds studied with the three biological protein targets.

Pharmacokinetics and drug-likeness predictions

The pharmacokinetics, drug-likeness, solubility, and Lipinski's properties of the investigated compounds are presented in Figure 8 and Supplementary Information Table S4-S9. In-silico pharmacokinetic analysis [38] is a useful tool to discover and design small molecules for a given target. The ligand is LoF, with a molecular weight < 500 g/mol, a number of hydrogen bond donors and acceptors < 5, a logP value < 5, and a molar refractivity < 140 [39, 40]. The ligand TPSA was 141.53 Å² indicating a potential for good absorption. The presence of < 5 rotatable bonds indicated that these compounds are more adaptable. The ligand was found to be water-soluble. The compounds' synthetic accessibility value was 7, indicating synthesis feasibility. None of the metal complexes followed the rules established for oral drug-likeness.

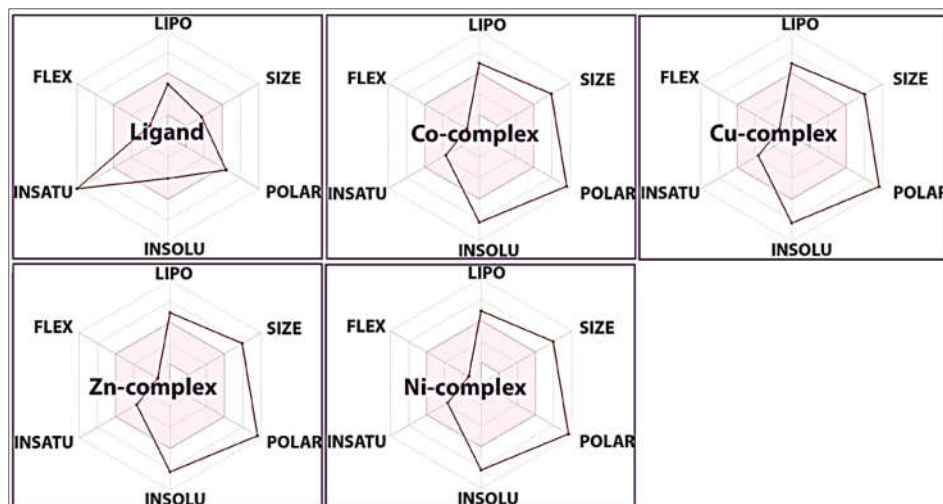


Figure 8. Pharmacokinetic properties of the compounds studied.

CONCLUSION

A series of benzothiazole-based azo ligand and its metal complexes were investigated. All the studied coordination compounds were shown to have metal ions in an octahedral environment. The isolated compounds showed significant antibacterial activity when tested against *S. aureus* and *E. coli*. However, zinc complex showed promising results. In addition, the metal-ligand complexes showed a high predictive binding affinity for the voltage-gated potassium channel KCNQ2 protein. Further studies are required to investigate the pharmaceutical potential of these compounds.

ACKNOWLEDGMENTS

The authors acknowledge the financial support through Researchers Supporting Project number (RSP2023R147), King Saud University, Riyadh, Saudi Arabia

REFERENCES

1. Bredas, J.-L.; Beljonne, D.; Coropceanu, V.; Cornil J. Charge-transfer and energy-transfer processes in pi-conjugated oligomers and polymers: a molecular picture. *Chem. Rev.* **2004**, 104, 4971-5004.
2. Staub, K.; Galina, A.; Levina, G.A.; Barlow, S.; Kowalczyk, T.C.; Lackritz, H.S.; Barzoukas, M.; Fort, A.; Marder, S.R. Synthesis and stability studies of conformationally locked 4-(diarylamino)aryl- and 4-(dialkylamino)phenyl-substituted second-order nonlinear optical polyenechromophores. *J. Mat. Chem.* **2003**, 13, 825-833.
3. McQuade, D.T.; Hegedus, A.H., Swager T.M. Signal amplification of a “turn-on” sensor: Harvesting the light captured by a conjugated polymer. *J. Am. Chem. Soc.* **2000**, 122, 12389-12390.
4. McQuade D.T., Pullen A.E., Swager T.M. Conjugated polymer-based chemical sensors. *Chem. Rev.* **2000**, 100, 2537-2574.

5. Abdullah; Akhtar, M.S.; Kim, E.-B.; Shin, H.-S.; Ameen, S. Justifying benzoselenadiazole acceptor core as organic semiconductor for stable bulk-heterojunction organic solar cells at ambient temperature. *J. Materiomics* **2021**, *7*, 51112-1121.
6. Abdullah; Kim, E.-B.; Akhtar, M.S.; Ameen, S. Highly stable bulk heterojunction organic solar cells based on asymmetric benzoselenadiazole-oriented organic chromophores. *Int. J. Energy Res.* **2022**, *46*, 7825-7839.
7. Derkowska-Zielinska, B.; Skowronski, L.; Kozłowski, T.; Smokal, V.; Kysil, A.; Biitseva, A.; Krupka, O. Influence of peripheral substituents on the optical properties of heterocyclic azo dyes. *Opt. Mater.* **2015**, *49*, 325-329.
8. Derkowska-Zielinska, B.; Gondek, E.; Pokladko-Kowar, M.; Kaczmarek-Kedziera, A.; Kysil, A.; Lakshminarayana, G.; Krupka, O. Photovoltaic cells with various azo dyes as components of the active layer. *Sol. Energy* **2020**, *203*, 19-24.
9. Nishihara, H. Combination of redox- and photochemistry of azo-conjugated metal complexes. *Coord. Chem. Rev.* **2005**, *249*, 1468-1475.
10. Zhou, Y.; Peng, P.; Han, L.; Tian, W.J. Novel donor-acceptor molecules as donors for bulk heterojunction solar cells. *Synth. Met.* **2007**, *157*, 502-507.
11. Bujak, K.; Orlikowska, H.; Maleckia, J.G.; Schab-Balcerzak, E.; Bartkiewicz, S.; Bogucki, J.; Sobolewska, A.; Konieczkowska, J. Fast dark cis-trans isomerization of azopyridine derivatives in comparison to their azobenzene analogues: Experimental and computational study. *Dyes Pigm.* **2019**, *160*, 654-662.
12. Tropp, J.; Ihde, M.H.; Crater, E.R.; Bell, N.C.; Bhatta, R.; Johnson, I.C.; Bonizzoni, M.; Azoulay, J.D. A sensor array for the nanomolar detection of azo dyes in water. *ACS Sens.* **2020**, *5*, 1541-1547.
13. Pervaiz, M.; Sadiq, S.; Sadiq, A.; Younas, U.; Ashraf, A.; Saeed, Z.; Zuber, M.; Adnan, A. Azo-Schiff base derivatives of transition metal complexes as antimicrobial agents. *Coord. Chem. Rev.* **2021**, *447*, 214128.
14. Gopi, C.; Sastry, V.G.; Dhanaraju, M.D. Synthesis, spectroscopic characterization, X-ray crystallography, structural activity relationship and antimicrobial activity of some novel 4-(5-(10-(3-N,N-dimethylamino)propyl)-10H-phenothiazine3-yl)-1,3,4-thiadiazole-2-yl)azo dye /Schiff base derivatives. *Future J. Pharm. Sci.* **2017**, *3*, 79-89.
15. Azam, M.; Al-Resayes, S.I.; Wabaidur, S.M.; Altaf, M.; Chaurasia, B.; Alam, M.; Shukla, S.N.; Gaur, P.; Albaqami, N.T.M.; Islam, M.S.; Park, S. Synthesis, structural characterization and antimicrobial activity of Cu(II) and Fe(III) complexes incorporating azo-azomethine ligand. *Molecules* **2018**, *23*, 813.
16. Ali, Y.; Hamid, S.A.; Rashid, U. Biomedical applications of aromatic azo compounds. *Mini Rev. Med. Chem.* **2018**, *18*, 1548-1558.
17. Saha, T.; Singha, S.; Kumar, S.; Das, S. Spectroscopy driven DFT computation for a structure of the monomeric Cu²⁺-curcumin complex and thermodynamics driven evaluation of its binding to DNA: Pseudo-binding of curcumin to DNA. *J. Mol. Struct.* **2020**, *1221*, 128732.
18. Sarangi, A.K.; Mahapatra, B.B.; Mohapatra, R.K.; Sethy, S.K.; Das, D.; Pintilie, L.; Kudrat-E-Zahan, M.; Azam, M.; Meher, H. Synthesis and characterization of some binuclear metal complexes with a pentadentate azodye ligand: An experimental and theoretical study. *Appl. Organomet. Chem.* **2020**, *34*, e5693
19. Mohapatra, R.K.; Sarangi, A.K.; Azam, M., El-ajaily, M.M.; Kudrat-E-Zahan, M.; Patjoshi, S.B.; Dash, D.C. Synthesis, structural investigations, DFT, molecular docking and antifungal studies of transition metal complexes with benzothiazole based Schiff base ligands. *J. Mol. Struct.* **2019**, *1179*, 65-75.
20. Al-Noor, T.H.; Mohapatra, R.K.; Azam, M.; Karim, L.K.A.; Mohapatra, P.K.; Ibrahim, A.A.; Parhi, P.K.; Dash, G.C.; El-ajaily, M.M.; Al-Resayes, S.I.; Raval, M.K.; Pintilie, L. Mixed-ligand complexes of ampicillin derived Schiff base ligand and Nicotinamide: Synthesis, physico-chemical studies, DFT calculation, antibacterial study and molecular docking

- analysis. *J. Mole. Struct.* **2021**, 1229, 129832.
21. Mohapatra, R.K.; Das, P.K.; Pradhan, M.K.; El-ajaily M.M., Das D., Salem H.F., Mahanta U., Badhei G., Parhi P.K., Maihub A.A., Kudrat E-Zahan M. Recent Advances in Urea- and Thiourea-Based Metal Complexes: Biological, Sensor, Optical, and Corrosion Inhibition Studies, *Comments Inorg. Chem.*, **2019**, 39, 127-187.
 22. Padilha, N.B.; Penteado, F.; Salomão, M.C.; Lopes, E.F.; Bettanin, L.; Hartwig, D.; Jacob, R.G.; Eder J. Lenardão, E.J. Peroxide-mediated oxidative coupling of primary alcohols and disulfides: Synthesis of 2-substituted benzothiazoles, *Tetrahedron Lett.*, **2019**, 60, 1587–1591.
 23. Huang, T.; Wu, X.; Yu, Y.; An, L.; Yin, X. A convenient synthesis of 2-acyl benzothiazoles/thiazoles from benzothiazole/thiazole and N,N'-carbonyldiimidazole activated carboxylic acids, *Tetrahedron Lett.*, **2019**, 60, 1667–1670.
 24. Yu, X.; Yin, Q.; Zhang, Z.; Huang, T.; Pu, Z.; Bao, M, Synthesis of 2-substituted benzothiazoles via the Brønsted acid catalyzed cyclization of 2-amino thiophenols with nitriles, *Tetrahedron Lett.*, **2019**, 60, 1964–1966.
 25. Sokolowska-Gajda, J.; Harold S. Freeman, H.S. A new medium for the diazotization of 2-amino-6-nitrobenzothiazole and 2-aminobenzothiazole, *Dyes Pigm.*, **1992**, 20, 137-145.
 26. Cao, H.W.; Zhao, J.F. Stability Constants of Cobalt(II) and Copper(II) Complexes with 3-[(o-Carboxy-p-nitrobenzene)azo]chromotropic Acid and Selective Determination of Copper(II) by Competition Coordination, *Cro. Chem. Acta*, **2003**, 76, 1-6.
 27. Wtter G., Ludwig N, Horst S., *Thermodynamics and statistical mechanics*, Springer-Verlag, 1995.
 28. Azam, M.; Wabaidur, S.M.; Alam, M.; Trzesowska-Kruszynska, A.; Kruszynski, R.; Al-Resayes, S.I.; Alqahtani, F.F.; Khan, M.R. Design, structural investigations and antimicrobial activity of pyrazole nucleating copper and zinc complexes, *Polyhedron*, **2021**, 195, 114991.
 29. Mohapatra, R.K.; Perekhoda, L.; Azam, M.; Suleiman, M.; Sarangi, A.K.; Semenets, A.; Pintilie, L.; Al-Resayes, S.I. Computational investigations of three main drugs and their comparison with synthesized compounds as potent inhibitors of SARS-CoV-2 main protease (Mpro): DFT, QSAR, molecular docking, and in silico toxicity analysis, *J. King Saud Univ. Sc.*, **2021**, 33, 101315.
 30. Kansiz, S.; Tolan, A.; Azam, M.; Dege, N.; Alam, M.; Sert, Y.; Al-Resayes, S.I.; Icbudak, H. Acesulfame based Co(II) complex: Synthesis, structural investigations, solvatochromism, Hirshfeld surface analysis and molecular docking studies. *Polyhedron* **2022**, 2018, 115762
 31. Shakir, M.; Azam, M.; Azim, Y.; Parveen, S.; Khan, A.U. Synthesis and physico-chemical studies on complexes of 1,2-diaminophenyl-N,N'-bis-(2-pyridinecarboxaldimine), (L): A spectroscopic approach on binding studies of DNA with the copper complex. *Polyhedron* **2007**, 26, 5513-5518.
 32. Firdaus, F.; Fatma, K.; Azam, M.; Shakir, M. Synthesis, spectroscopic, thermal, and antimicrobial studies of tetradentate 12 and 14 member Schiff bases and their complexes with Fe(III), Co(II), and Cu(II). *J. Coord. Chem.* **2010**, 63, 3956-3968.
 33. Nakamoto K. *Infrared and Raman Spectra of Inorganic and Coordination Compounds*, 4th ed., Wiley Interscience: New York; **1986**.
 34. Azam, M.; Dwivedi, S.; Al-Resayes, S.I.; Adil, S.F.; Islam, M.S.; Trzesowska-Kruszynska, A.; Kruszynski, R.; Lee, D.-L. Cu(II) salen complex with propylene linkage: An efficient catalyst in the formation of CX bonds (X = N, O, S) and biological investigations. *J. Mol. Struct.* **2017**, 1130, 122-127.
 35. Parang, K.; Till, J.H.; Ablooglu, A.J.; Kohanski, R.A.; Hubbard, S.R.; Cole, P.A. Mechanism-based design of a protein kinase inhibitor. *Nat. Struct. Biol.* **2001**, 8, 37-44.
 36. Li, X.; Zhang, Q.; Guo, P.; Fu, J.; Mei, L.; Lv, D.; Wang, J.; Lai, D.; Ye, S.; Yang, H.; Guo, J. Molecular basis for ligand activation of the human KCNQ2 channel. *Cell Res.* **2021**, 31, 52-61.

37. Coleman, J.A.; Green, E.M.; Gouaux, E. X-ray structures and mechanism of the human serotonin transporter. *Nature* **2016**, 532, 334-339.
38. Savale, R.U.; Bhowmick, S.; Osman, S.M.; Alasmay, F.A.; Almutairi, T.M.; Abdullah, D.S.; Patil, P.C.; Islam, M.A. Pharmacoinformatics approach-based identification of potential Nsp15 endoribonuclease modulators for SARS-CoV-2 inhibition. *Arch. Biochem. Biophys.* **2021**, 700, 108771.
39. Lipinski, C.A. Drug-like properties and the causes of poor solubility and poor permeability. *J. Pharmacol. Toxicol. Methods* **2000**, 44 235-249.
40. Lipinski, C.A. Lead- and drug-like compounds: the rule-of-five revolution. *Drug Discov. Today Technol.* **2004**, 1, 337-341.